8-6-2008

Impact of Climate Change on Irrigation Water Availability, Crop Water Requirements and Soil Salinity in the SJV, CA

Jan Hopmans

Edwin P. Maurer
Santa Clara University, emaurer@scu.edu

Abstract:
We examine potential regional-scale impacts of global climate change on sustainability of irrigated agriculture, focusing on the western San Joaquin Valley in California. We consider potential changes in irrigation water demand and supply, and quantify impacts on cropping patterns, groundwater pumping, groundwater levels, soil salinity, and crop yields. Our analysis is based on archived output from General Circulation Model (GCM) climate projections through 2100, which are downscaled here to the scale of the study area (~30 km across). We account for uncertainty in GCM climate projections by considering output from two different GCM's, each using three greenhouse gas emission scenarios. Significant uncertainty in projected precipitation translates into uncertainty of future water supply, ranging from an increase of 10% to a decrease of 30% in 2100. On the other hand, temperature projections are much less variable, resulting in consistent projections of crop water demand for all climate change scenarios. Crop water demand is expected to change very little, due to compensating effects of rising temperature on evaporative demand and crop growth rate. Reductions in surface water supply are projected to be offset by groundwater pumping and land fallowing. Simulations of subsurface flow and salt transport with a regional-scale hydro-salinity model suggest a small expansion in salt-affected area, compared to current conditions. However, in all scenarios salinity is expected to increase in downslope areas, thereby limiting crop production. This is especially significant given an anticipated demand-driven switch to high-value, salt-sensitive crops. Results show that technological adaptation, such as improvements in irrigation efficiency, may partly mitigate these effects.

Impact of Climate Change on Irrigation Water Availability, Crop Water Requirements and Soil Salinity in the SJV, CA

Jan W. Hopmans (University of California, Davis; jwhopmans@ucdavis.edu), and
Edwin P. Maurer (Santa Clara University; EMaurer@scu.edu)

UC Water Resources Center Technical Completion Report Project SD011

Submitted: June, 2008

1. Abstract

We examine potential regional-scale impacts of global climate change on sustainability of irrigated agriculture, focusing on the western San Joaquin Valley in California. We consider potential changes in irrigation water demand and supply, and quantify impacts on cropping patterns, groundwater pumping, groundwater levels, soil salinity, and crop yields. Our analysis is based on archived output from General Circulation Model (GCM) climate projections through 2100, which are downscaled here to the scale of the study area (~30 km across). We account for uncertainty in GCM climate projections by considering output from two different GCM's, each using three greenhouse gas emission scenarios. Significant uncertainty in projected precipitation translates into uncertainty of future water supply, ranging from an increase of 10% to a decrease of 30% in 2100. On the other hand, temperature projections are much less variable, resulting in consistent projections of crop water demand for all climate change scenarios. Crop water demand is expected to change very little, due to compensating effects of rising temperature on evaporative demand and crop growth rate. Reductions in surface water supply are projected to be offset by groundwater pumping and land fallowing. Simulations of subsurface flow and salt transport with a regional-scale hydro-salinity model suggest a small expansion in salt-affected area, compared to current conditions. However, in all scenarios salinity is expected to increase in downslope areas, thereby limiting crop production. This is especially significant given an anticipated demand-driven switch to high-value, salt-sensitive crops. Results show that technological adaptation, such as improvements in irrigation efficiency, may partly mitigate these effects.

2. Introduction and problem statement

We present the methodology and results of a quantitative analysis of the potential effects of climate change on the sustainability of irrigated agriculture in the western San Joaquin Valley, CA. The analysis is done at the regional scale (study area ~1400 km^2), as shown in Figure 1, and for a time horizon extending to the year 2100. An earlier study that focused on the modeling of historical changes in soil and groundwater salinity since the 1940's was published by Schoups et al. (2005), and concluded that irrigated agriculture has contributed significantly to deep groundwater salinity, and that gypsum dissolution was the principal salt source. A preliminary report of the presented modeling results with the focus on the future is available at Hopmans and Maurer (2007).

The analysis is based on projected global changes in greenhouse gas (GHG) emissions, and resulting changes in temperature and precipitation as simulated by global climate models (GCM). Uncertainty in climate change predictions is handled through the use of three GHG emission scenarios and two GCM's. These data serve as input for a

downscaling procedure to determine changes in meteorological conditions (temperature, precipitation, and evapotranspiration) at the regional scale of this study. Resulting impacts on water supply and crop water demand are calculated for irrigated agriculture in the study area. Crop response includes changes in crop water demand due to changing atmospheric conditions. We considered future changes in potential crop ET rates caused by (i) increased atmospheric CO_2 levels, (ii) increased reference ET, and (iii) increased air temperatures.

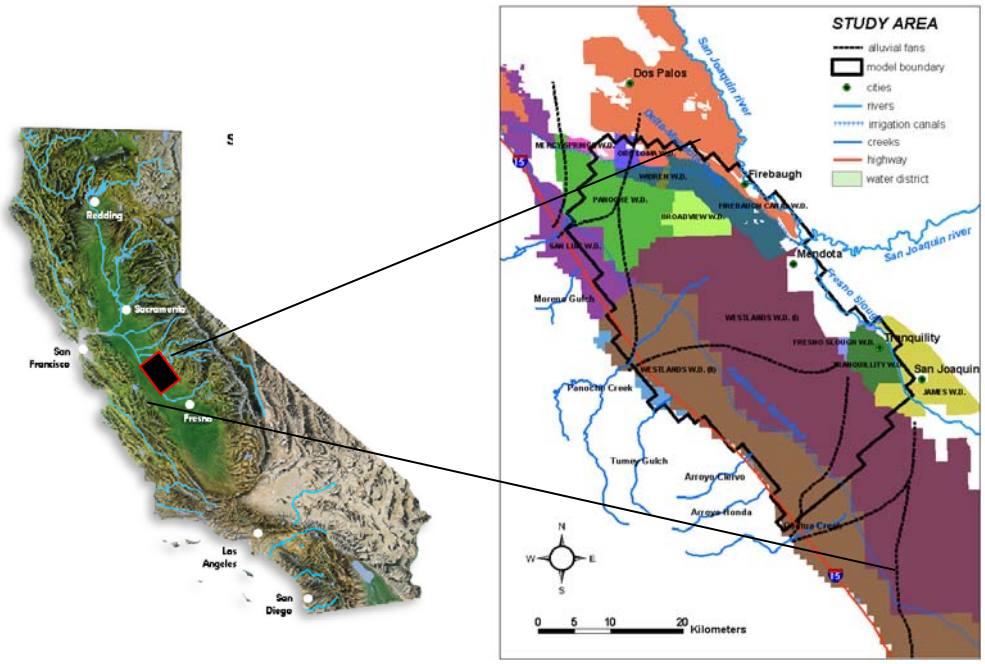

Figure1. Location of the ~1400 km^2 study area in the western San Joaquin Valley, California.

We considered the following possible management responses to changes in surface water supplies and crop ET: (i) land fallowing and retirement, (ii) changes in cropping patterns, (iii) groundwater pumping, and (iv) technological adaptation. We predicted temporary land fallowing assuming it is inversely related to surface water supply, as indicated by historical fallowing during droughts in the study area. These results are used in turn to assess effects on agricultural water and crop management by quantifying potential changes in groundwater pumping, crop choices, and water use efficiency. In the final step, the climate-change induced changes in crop ET, surface water supply, and groundwater pumping were used as input into a hydro-salinity model of the study area to assess resulting impacts on groundwater levels, land subsidence, soil salinity, and crop yields. This was done for 8 climate change scenarios, including a no-climate-change scenario and one that assumes a uniform irrigation efficiency of 90% by technological adaptations. Although scenarios differed significantly in the amount of groundwater applied, and the simulated extent of shallow water tables, soil salinity predictions do not vary greatly between scenarios. Wet scenarios resulted in less groundwater pumping, whereas the dry scenarios projected increased groundwater pumping, causing downward hydraulic gradients and lowering of shallow water tables.

The recycling of groundwater by pumping exacerbates the groundwater salinity problem because of downward mobilization of dissolved gypsum.

3. Objectives

An earlier study that focused on the modeling of historical changes in soil and groundwater salinity since the 1940's was published by Schoups et al. (2005). It was shown that soil salinization is related to (i) groundwater use during periodic droughts and (ii) development of shallow water tables due to excessive surface water irrigation. In addition, groundwater salinity was shown to increase due to leaching of salts from agriculture and continued dissolution of gypsum present in the alluvial deposits. The general objective of the proposed study is to investigate how these trends will continue into the 21st century, particularly in the light of expected climate change. Specifically, GCM output was downscaled to the Schoups et al. (2005) model domain, and the hydrosalinity model was applied to evaluate the impact of climate change on irrigated agriculture in the 21st century for the SJV.

4. Procedures

The general methodology is presented schematically in Figure 2. We consider three increased greenhouse gas emission scenarios and study the potential impacts on the agrohydroclimatological conditions in the region up to 2100. In particular, the analysis is broken down into four main impact areas: (i) climate response, (ii) crop response, (iii) agricultural water and crop management response, and (iv) hydrologic response.

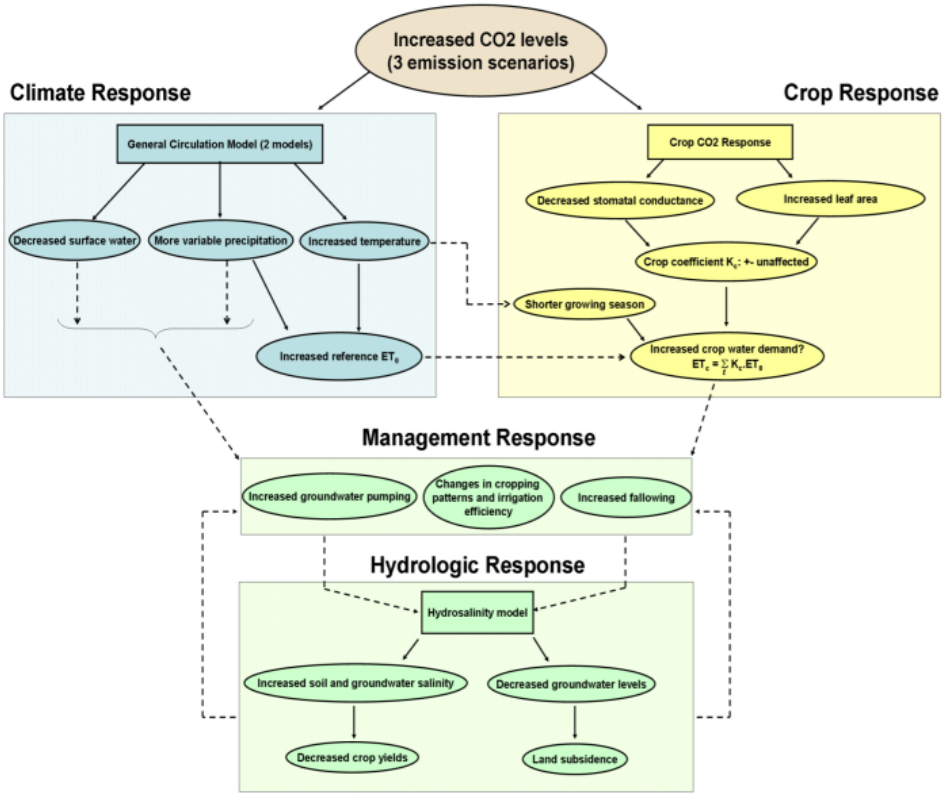

Figure 2. Overview of the methodology for assessing potential climate change impacts on irrigated agriculture.

4.1. Climate Response

We considered three future greenhouse gas (GHG) emission scenarios: SRES B1 (low), A2 (mid-to-high) and A1fi (high). These scenarios bracket a large part of the range of IPCC's nonintervention future emissions projections, with atmospheric concentrations of CO_2 for B1, A2, and A1fi reaching 550 ppm, 850 ppm and 970 ppm, respectively by 2100. For each of the three GHG emission scenarios we calculate the effect of increased atmospheric CO_2 levels on future climatic variables, i.e. daily precipitation, air temperature, and reference evapotranspiration, at the regional-scale of this study.

We use the two General Circulation Models (GCMs) used by Hayhoe et al. (2004): the National Center for Atmospheric Research-Department of Energy Parallel Climate Model (PCM, Washington et al., 2000) and the U.K. Met Office Hadley Centre Climate Model version three (HadCM3, Gordon et al., 2002). Using the definition of GCM climate sensitivity as the increase in global mean air temperature projected by the model after reaching equilibrium conditions with doubled atmospheric CO_2 (IPCC, 2001), PCM and HadCM3 have sensitivities of 2.1 and 3.3, respectively IPCC (2001). Both GCMs are fully coupled atmosphere-ocean models that maintain a relatively stable climate over long control simulations without imposed adjustments. Both also simulate realistic El Niño-Southern Oscillation (ENSO) variability, important for California climate. The GCM simulations using the B1 and A1fi scenarios are those described by Hayhoe et al. (2004); those using the A2 scenario are described by Maurer (2006). The output of the two GCMs is used to extract precipitation and air temperature predictions for California at a spatial resolution of about 300 km for the three GHG emission scenarios.

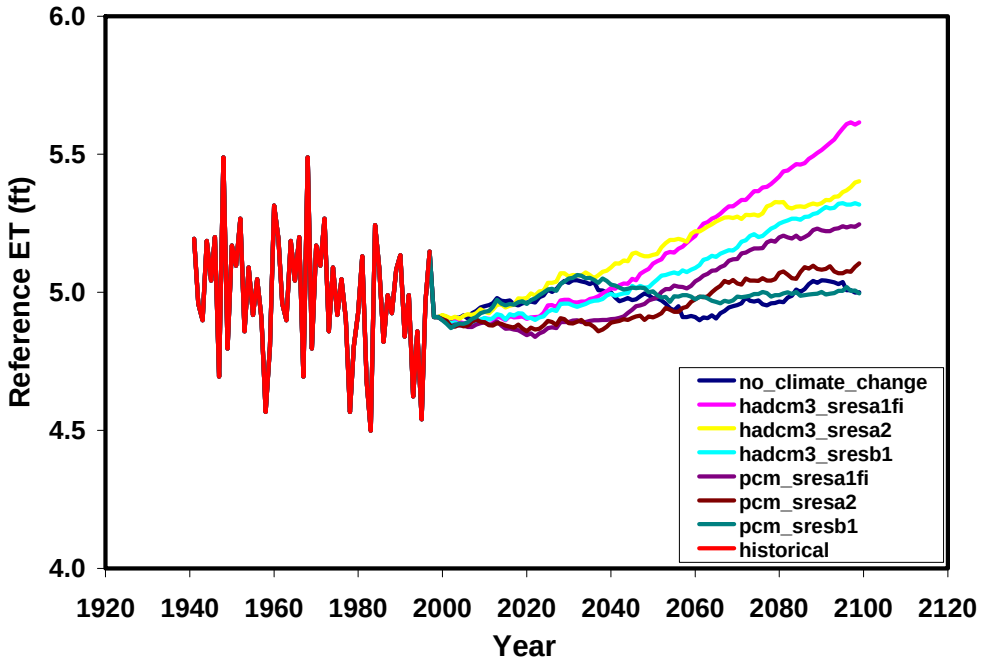

Figure 3. Predicted, annual reference ET for 6 climate change scenarios. Plotted values: annual totals from 1941 to 1997, and 30-year moving averages from 1998 to 2099. For example, the plotted value for 1998 corresponds to the average for 1969-1998.

The original data consist of observed (or projected) surface meteorological data of precipitation and temperature. Because surface observations of wind speed are sparse and are biased toward certain geographical settings (e.g., airports), daily 10-m wind fields were obtained from the NCEP/NCAR reanalysis (Kalnay et al., 1996), and interpolated to a fine grid resolution from the T62 Gaussian grid (approximately 1.9° square) to the 1/8° grid using linear interpolation. Wind speed is translated from a 10 meter height to 2 meters by assuming a logarithmic wind profile. Established relationships are used to determine vapor pressure, and incoming longwave and shortwave radiation using these data, e. g. Maurer et al, (2002), studies of large-scale drought (Andreadis and Lettenmaier, 2006), California river basin hydrology (Yates et al., 2005), and climate change impacts on California (Cayan et al., 2006). The standardized reference crop evapotranspiration, for a short, 0.12 m grass was computed using the ASCE-EWRI standardized equation (ASCE-EWRI, 2004; Shuttleworth, 1993).

The spatial resolution of the GCM output used in this study is roughly 250-325 km, which is too large. We applied the empirical statistical downscaling method, developed by Wood et al. (2002) to apply the GCM model results to our model domain. This was done by bias-correcting of historical probability density functions (PDF) of monthly GCM projections of precipitation and temperature during the 1960-1999 climate period, by comparison with observed data for the same period aggregated to the GCM scale. The bias-correction was performed by mapping, one month at a time, the GCM PDF to that of the observed data, resulting in the corrected GCM data statistically matching the observed data. The same PDF mapping was applied to 21st century GCM projections, so that while the statistics of observations are reproduced for the 20th century, both the mean and variability of future climate can evolve according to GCM projections. The combined bias correction/spatial downscaling method has been shown to compare favorably to different statistical and dynamic downscaling techniques (Wood et al., 2004). This approach was validated through the excellent agreement between historical GCM-downscaled and observed meteorological variables for our study area, i.e. temperature, precipitation, and reference ET (Fig. 3).

Since a detailed analysis of potential future changes in water supplies was beyond the scope of this study, we relied on the results of Vicuna et al. (2006) to estimate water supplies for each of our six climate change scenarios. Our methodology was based on the observation that long-term changes in precipitation explain most of the variance in expected surface water deliveries. Vicuna et al. (2006) studied the impacts of climate change on surface water supplies to irrigated agriculture in California's Central Valley. First, they used downscaled GCM output from two GCMs (PCM and HadCM3), combined with two GHG emission scenarios (low (B1) and high (A1fi)), as input into a hydrologic model (the VIC model) to calculate impacts of climate change on natural runoff from the Sierra Nevada mountains. Subsequently they assessed the impact of these changes in runoff on reservoir storages and surface water supplies for irrigation using the CalSim II water planning model. They predicted long-term changes in surface water supplies by the end of the century ranging from a decrease of about 30% to an increase of about 5% relative to historical water supplies. The largest decreases were obtained with the high GHG emission scenario (A1fi) for both GCMs (Vicuna et al., 2006). Thus, also our approach used long-term precipitation in the study area as a proxy for long-term changes in future surface water supply. As a final result, we generated future water supply scenarios that (i) account for long-term trends in surface water supply as a

function of long-term precipitation shifts, and at the same time (ii) preserve the short-term statistical properties (variation, correlation) of current and historical water supply for each water district. Trends in water supply for the six climate change scenarios are presented in Fig. 4, of which the relative magnitudes between scenario's reflect differences in precipitation forecasts between scenarios.

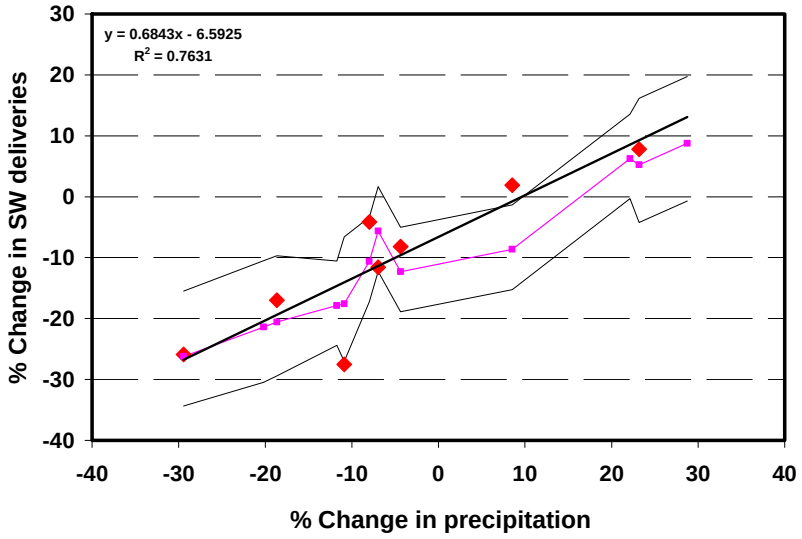

Figure 4. Predicted changes in surface water supply (as % of average surface water supply during 1973-1997) as a function of predicted changes in precipitation (as % of average precipitation). Red diamonds are data points based on the results of Vicuna et al. (2006), for four of the six climate change scenarios considered here (combination of a GHG emission scenario and a GCM), and for two future time periods, namely 2020-2049 and 2070-2099. The dark solid line is a regression through these data points. The pink curve is based on simulated supply time-series averaged over all water districts, and the two solid curves show minimum and maximum values obtained for district water supply.

4.2. Crop response

We are concerned with predicting the effects of climate change on crop growth and crop water demand (ET). Seasonal potential crop ET or ET_p is calculated as follows,

$$ET_p = \sum_{d=1}^{d_s} k_c ET_0 \qquad , \quad (1)$$

where ET_0 is daily reference ET (mm), k_c is daily crop coefficient (-), and the summation is over the duration d_s (days) of the crop growing season. We consider future changes in potential crop evapotranspiration (ET_p) rates caused by (i) increased atmospheric CO_2 levels (Fig. 1) and (ii) increased air temperatures. The direct effect of increased atmospheric CO_2 on crop growth and ET has been studied extensively by means of so-called FACE (Free-Air CO_2 Enrichment) experiments for various crops (Ainsworth and Rogers, 2007). In general, increased CO_2 results in a decrease in stomatal conductance leading to less transpiration. However, this effect is balanced by a corresponding increase in canopy temperature and an increase in leaf area. Therefore, the overall effect of increased CO_2 levels depends on the magnitude of these competing mechanisms. As a first approximation we assumed that the direct effect of increased levels of CO_2 on crop ET is negligible. In other words, we use current crop coefficients k_c in Eq. (1) to calculate

crop ET (Snyder et al., 1989), and ignored possible future changes in k_c due to climate change

Predicted increases in air temperature may result in faster plant development and therefore shorter growing seasons. On the other hand, extremely high summer temperatures may negatively impact crop growth, as many crops suffer heat stress beyond an optimal temperature range. The effect of temperature on crop development is typically quantified using thermal units or degree-days (Snyder, 1985; Ritchie and NeSmith, 1991), such that the length of crop development stages is expressed in degree-days instead of days. Degree-days were accumulated throughout the growing season and used to express crop development stages in degree-days instead of days. We calculated the length in degree-days of the various crop development stages for 25 crops in the study area using historical temperature data. Subsequently, the calculated degree-days for crop development were used together with predicted average daily temperatures to compute crop growth rates and growing seasons for the six climate change scenarios. This procedure resulted in faster or slower crop development, and hence shorter or longer growing seasons, depending on the predicted increase in temperature in each scenario compared to current conditions. Predicted shortening or lengthening of crop growing seasons in turn affects computed seasonal crop water requirements (crop ET) through the summation of crop water demand over the growing season in Eq. (1). The resulting predicted seasonal crop water demand (ET_p) varied between crops, but generally led to a decreased or unchanged seasonal crop water requirements for most crops as the increase in crop water demand due to increased reference ET (the indirect CO_2 effect) was mostly offset by faster crop development due to increased temperature. An exception is the high-emission scenario with the hadcm3 climate model, which is characterized by the largest temperature increases and results in delayed crop growth due to heat stress and therefore a pronounced increase in crop ET for both cotton and tomato.

4.3. Management response

We can put the various management decisions into context by considering the seasonal water balance for a water district in the study area,

$$IR = SW + GW \qquad , \qquad (2)$$

where *IR* is irrigation requirement, i.e. the volume of water needed to irrigate all crops, *SW* is the surface water supply, and *GW* is the volume of pumped groundwater. Total irrigation requirement can also be expressed as the sum of water needs for all crops,

$$IR = \sum_{cr} A_{cr} \frac{ET_{cr} - P_{cr}}{IE_{cr}} \qquad , \qquad (3)$$

where ET_{cr} is crop water demand, which is equal to ET_p in Eq. (1) when no water or salinity stress occurs, P_{cr} is effective precipitation, and IE_{cr} is irrigation efficiency, which accounts for conveyance and leaching losses, and A_{cr} is areal crop fraction. For the management response we consider the amount of surface water supply *SW* a given that cannot be changed through management in the study area, and evaluate how the other two terms in Eq. (2), *GW* and *IR*, can be managed to close the water balance.

A first option to balance cuts in surface water supplies is to increase groundwater pumping *GW*. There are however several potentially limiting factors associated with this strategy, such as (i) the available pumping capacity (number of wells), (ii) the quality of

local groundwater, (iii) the cost of pumping, and (iv) the risk of secondary effects such as land subsidence. Under the section "hydrologic response" we will consider the effects of groundwater pumping on soil salinity and crop yields, and on land subsidence. A second group of measures to deal with surface water supply cuts aim to reduce total irrigation requirement *IR*. This can be done by (i) fallowing land, (ii) changing the crop mix by switching to crops with lower water demands, (iii) developing new water-efficient and heat-resistant cultivars, and (iv) improving irrigation efficiency and technology. The first two responses can be classified as actual management responses in the sense that they do not require any technological or infrastructural change, whereas the last two responses involve infrastructural changes in irrigation technology and crop cultivars. A common approach to including management decisions, i.e. human behavior, into predictive simulations is to employ optimization techniques and assume that future management will try to maximize (or minimize) some objective function, e.g. profit from agricultural production. Such an approach is outside the scope of our work, and given the large uncertainties associated with predicting future markets we will instead consider a couple of alternative management scenarios to bracket a range of possible management outcomes.

4.3.1. Land fallowing and retirement

In order to assess possible future land fallowing, we used historical data. For example, the study area experienced a severe drought in the early 1990's, during which surface water supplies where reduced by up to 75% and up to 50% of irrigable land was temporarily fallowed. By analyzing observed correlations between historical surface water supplies and fallowing, for each water district, we derived functional relationship (linear regression) between fallowing and surface water deliveries for the 1988-1997 period, and used these for projecting fallowing between climate change scenarios. We also consider permanent retirement of agricultural land due to excessive soil salinization. Recently almost 100,000 acres of salt-affected land was retired in Broadview and Westlands Water Districts (WWD). These retired areas correspond to downslope agricultural land affected by shallow water tables and limited drainage. A direct consequence of land retirement in these downslope areas is that surface water supplies are freed up and transferred to upslope areas in Westlands Water District. We accounted for land retirement in the study area in all our predictive simulations with the hydrosalinity model.

4.3.2. Changes in cropping patterns

Alternatively, reduced surface water availability can be managed by shifting to more water-efficient, high-value crops. Looking at changes in cropping patterns during the recent drought in the early 1990s, such a shift is not directly evident. The absence of significant cropping shifts in the period 1988-1997 is probably due to the fact that the drought only lasted a couple of years, which is not enough time for farmers to adapt. Furthermore, cropping choices are potentially also influenced by several other factors such as crop price reliability and crop demand. Howitt et al. (2003) studied potential future changes in cropping patterns in California as affected by changes in crop demand and climate change. They conclude that changes in the 2100 cropping pattern are mainly driven by the shift in the demand, with little differences in predicted cropping patterns between various climate change scenarios. In order to evaluate the effects of a shift in cropping patterns, we calculated crop ET, irrigation water demand, and groundwater

pumping for two scenarios: (i) a demand-driven shift to high-value crops, as suggested by Howitt et al. (2003), and (ii) no change in cropping patterns. Comparing the two scenarios we conclude that the crop shift has a negligible effect on crop ET. Hence, from a hydrologic point of view, the potential crop shift is insignificant. However, to the extent that these high-value crops are less salt tolerant, it is important to evaluate the effects of soil salinity on crop yields for both crop scenarios. In view of this result, we assumed that cropping patterns will not changed significantly and for each district average historical crop acreages (1988-1997) were used as a basis for calculating future crop acreages, which were adjusted according to the calculated fallowed acreages. Cropping shifts may also occur through the effect of climate change (direct CO_2 effect, temperature) on crop yields. Current research results point to increased yields under elevated CO_2 conditions, whereas temperature increases may negatively impact crop yields.

4.3.3. Groundwater pumping

As surface water supplies decrease they will partly be substituted for by pumping groundwater. The amount of groundwater pumping is estimated based on (i) the predicted water requirements of each crop ET_p, (ii) the predicted crop acreages (including fallowing), (iii) the predicted changes in surface water supplies, and (iv) the predicted precipitation rates. If irrigation requirements cannot be met by surface water supplies and within-season precipitation, then the difference is estimated to equal groundwater pumping. Irrigation requirements include water needed for flushing out salts. This is accounted for by means of an irrigation efficiency parameter, which varied as a function of predicted groundwater depths (irrigation efficiency is higher under shallow water table conditions with limited drainage). Two potential adaptations to future climate change are considered, namely (i) improvements in irrigation technology, and (ii) development of new crop cultivars. Improvements in irrigation technology can result in increases in irrigation efficiency and smaller water losses at the field scale. This can also be achieved by improving irrigation practices using current technology. In our analysis these two measures are indistinguishable. We simulated adaptation by considering a management scenario with a higher IE for all crops of IE = 0.9. The results for the various climate change scenarios are presented in Fig. 5.

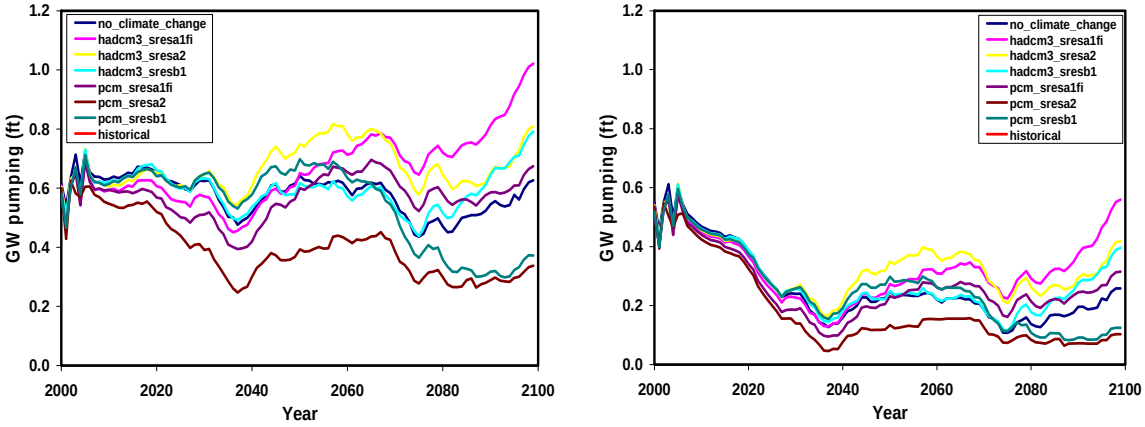

Figure 5. Predicted groundwater pumping (30-year averages) in the study area (excluding retired land) for 6 climate change scenarios, assuming various future irrigation efficiencies (IE): (a) IE values of 0.8, 0.72, and 0.65, as a function of water table depth, and (b) uniform IE of 0.9.

4.4. Hydrologic response

The original model of Schoups et al. (2005) was extended to include the confined sub-corcoran aquifer. Since most groundwater pumping occurs from this aquifer, confined heads are expected to change considerably as a function of pumping, which in turn affects vertical gradients and flow through the Corcoran clay. The historical simulations of Schoups et al. (2005) relied on observed heads in the confined aquifer to quantify flow through the Corcoran clay, thereby eliminating the need for confined flow simulation. However, in order to estimate potential changes in subsurface hydrology, confined flow needs to be simulated as well. We followed Belitz and Phillips (1993) in representing the confined aquifer by a 1,000 ft thick layer. In addition, we explicitly represent the Corcoran clay in the model, using a layer of variable thickness, given by mapped thicknesses of Corcoran clay (varies between 20 and 200 ft). Inclusion of the confined aquifer changed the model response for historical conditions. Therefore, the model was manually recalibrated to historical conditions, using a series of simulation runs and changing permeability values such that observed changes in groundwater levels (water tables and confined water levels), and soil salinity in the 1990s was approximately reproduced. All other parametric model input values (e.g. hydraulic properties) were adopted from the hydrosalinity model developed by Schoups et al. (2005). As a first step, the hydrosalinty model was run for historical conditions from 1941 to 1997. The 1997 output (groundwater levels, salt and ion concentrations, mineral contents) was used as initial conditions for the predictive runs, to simulate hydrological and salinity variables through 2099. Following Schoups et al. (2005), boundary conditions at the land surface consist of annual infiltration rates and evapotranspiration rates for each cell of the numerical grid, with crop maps derived from projected annual crop acreages for each water district for the entire simulation period. Annual infiltration rates for each grid cell were calculated as the sum of annual precipitation and irrigation water delivery (surface water and groundwater). Surface water deliveries were distributed spatially based on irrigation requirements between grid cells (a function of crop type and irrigation efficiency). Groundwater use was calculated as the difference between irrigation requirement and water availability (surface water and within-season precipitation). Under current conditions, groundwater flows eastward out of the eastern model boundary towards the Fresno Slough/San Joaquin river. The rate of lateral groundwater discharge depends on groundwater levels just east of the model domain. Due to a lack of information, groundwater levels at the eastern domain boundary were kept constant at their 1990s observed levels. Following Belitz et al. (1993), no flow is assumed to occur between the confined aquifer and underlying geological layers.

5. Results

We compare projected conditions for the various climate change scenarios, and compare with current conditions. In the following, focus is on, respectively, projected groundwater levels, soil and groundwater salinity, crop yields, and land subsidence. Finally, conclusions are drawn regarding significance of the results for sustainability of agricultural production in the area. All scenarios account for permanently retired land (taken out of production).

5.1. Groundwater level Projection

Figure 6 compares historical with projected changes in the extent of the area affected by shallow water table (within 7 ft of land surface). In the absence of climate change through

2100, no significant trends are projected in shallow water table extent. This is somewhat surprising given that part of the area has been retired from agricultural production and irrigation. Considering the results for the no-climate-change scenario, the simulations showed some decrease of groundwater levels in retired areas (e.g. in Broadview Water District). However, this is compensated for by a further upslope (westward) migration of the area with shallow water tables.

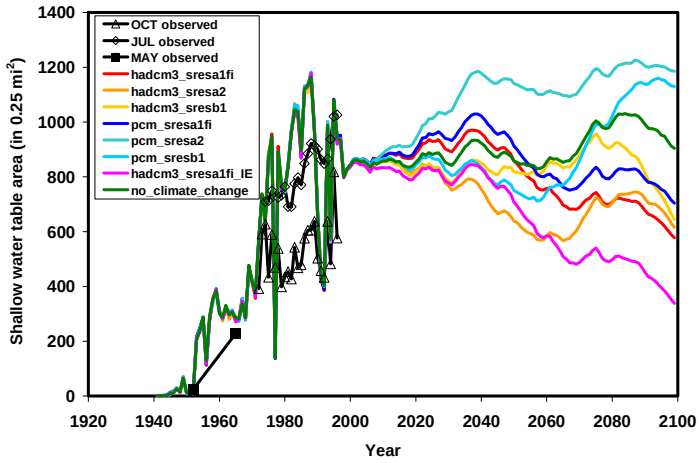

Figure 6. Historically observed/simulated and projected extent of shallow water table area (within 7 ft of land surface) for 8 climate change scenarios. Results are shown as either annual values (before 1998) or 30-year averages (after 1998).

5.2. Soil Salinity Projection

Figure 7 summarizes the simulated soil salinity results. Historical simulations (1940-1998) show an initial decrease in salinity as soils are reclaimed by irrigation. This is followed by a period of renewed salinization (starting in 1970's), due to importation of surface water, leading to rising water tables, and drainage problems. These dynamics were already described in Schoups et al. (2005). Though results of historical reconstruction deviate somewhat from those presented in Schoups et al. (2005), the main conclusions and simulated dynamics remain unaltered.

Salinity projections are much less variable across climate change scenarios, and remain constant, except tor the one scenario with the largest temperature increase projections (Hadcm3-a1fi). Hence, there appears to be an upper limit on the area affected by soil salinity, limited by the badly drained areas in the eastern half of the study area. The western half of the study area remains well drained, due to greater topographic gradients there and coarser alluvial deposits. A comparison of groundwater level with soil salinity maps showed that the presence of shallow water tables area, but without significant salinization. In those cases further rise of and evaporation from shallow water tables is prevented by sufficient drainage to deeper groundwater layers.

5.3. Groundwater Salinity Projection

Degradation of groundwater quality was evaluated by computing excessive salt loads to groundwater by downward recharge. Results of simulated and projected salt loads to groundwater are presented in Figs. 8 and 9. Temporal evolution of cumulative salt loads

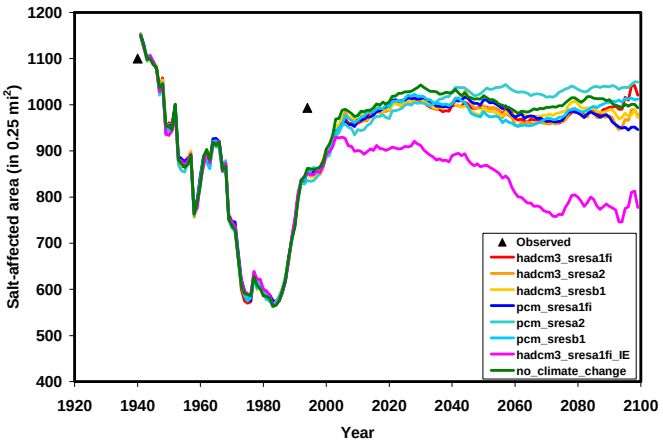

Figure 7. Historically observed/simulated and projected extent of salt-affected area (average EC_e more than 4 dS/m within top 7 ft) for 8 climate change scenarios. Results are shown as annual values throughout the entire period.

to groundwater (Fig. 8) showed an initially sharp increase due to irrigation development in the 1940's and 50's, with sole reliance on groundwater pumping in the early 1900's. The rate of increase slows down in the 1970s and 1980s due to the switch to fresh surface water. This lower rate of increase persists throughout the 21st century for the no-climate-change scenario. Wetter scenarios (pcm-sresa2 and pcm-sresb1) exhibit a lower rate of increase, whereas dry scenarios (e.g. hadcm3-sresa1fi) with a greater amount of groundwater pumping increase faster. The slower rate in wet scenarios is also caused by the larger simulated extent of areas with groundwater discharge into the root-zone (i.e. "negative" salt loads, where the net salt flux is pointed upwards into the root-zone). This is clearly indicated by the maps in Figure 9, where blank areas represent areas of groundwater discharge into the root-zone. These are also areas of greatest soil salinity and lowest crop yields. Salt loads to groundwater are greatest in the western half of the study area, as indicated by blue colors. These are areas where soil salinity is controlled by salt leaching from the root-zone. These salts may move down to producing aquifers, eventually affecting salinity of pumped groundwater, although this process may take hundreds of years.

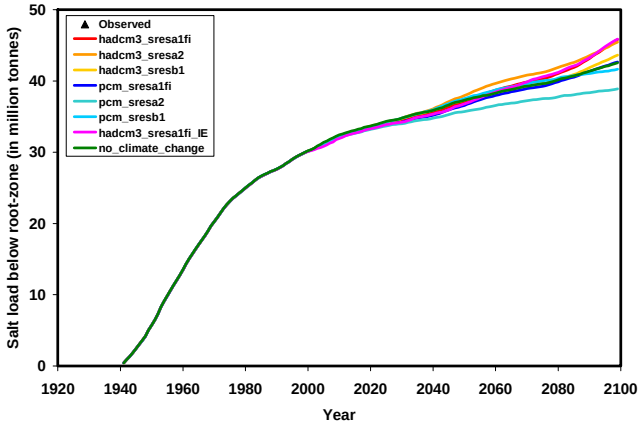

Figure 8. Simulated and projected cumulative values of total salt load below the root-zone. Summation occurs over all grid cells in the study area, and includes both positive values, where salts move into groundwater, and negative values, where salts discharge from groundwater into the root-zone.

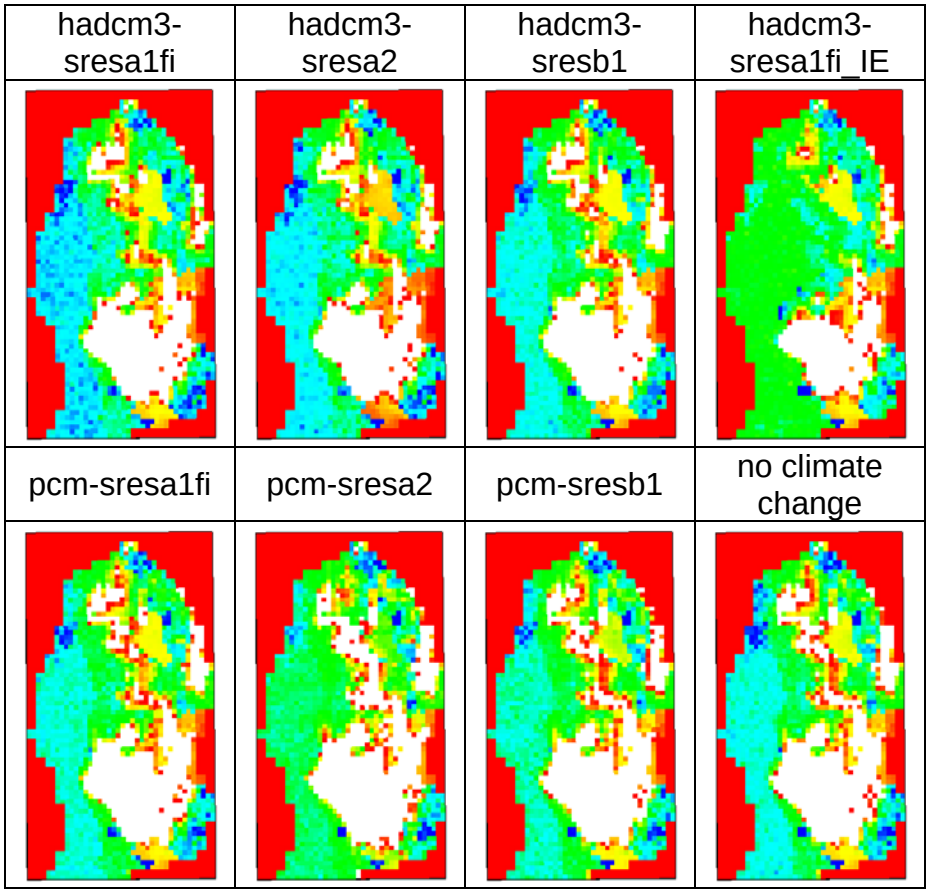

Figure 9. Maps of projected salt loads below the root-zone (2010-2100). Blank areas represent negative salt loads, where salts discharge from groundwater into the root-zone. High to low values are represented by color scale blue-green-yellow-red.

5.4. Land Subsidence Projection

A potential negative effect of reduced surface water supplies under climate change, is that increased groundwater pumping may lead to land subsidence. Historically, prior to the construction of the California Aqueduct in the 1960's and the importation of surface water from northern California, irrigated agriculture relied heavily on locally pumped groundwater, which has caused substantial land subsidence of up to 30 ft locally during 1926-1972 (Ireland et al., 1984). Since most groundwater pumping occurred from the confined aquifer, this is also where most compaction has taken place. With the replacement of groundwater by imported surface water in the late 1960's, groundwater levels in the confined aquifer have recovered and land subsidence has been halted. However, land subsidence is still a concern during times of increased groundwater pumping, as observed during droughts in 1977 and 1987-1992, and as may happen due to reduced surface water supplies under climate change.

Land subsidence can be predicted by coupling a subsidence model to regional groundwater flow, accounting for both elastic (recoverable) and inelastic (irrecoverable)

compaction and land subsidence, and applied the model to assess potential land subsidence for a couple water management scenarios. Results showed that a scenario of increased groundwater pumping, originally proposed by Belitz and Phillips (1995) to lower shallow water tables in the area, produces significant inelastic compaction in the next 30 years. Hence, land subsidence is an important factor to consider under climate change.

The purpose was to determine approximate estimates of potential future land subsidence for the 8 climate change scenarios. In particular, we are concerned with inelastic compaction and land subsidence, which may occur when hydraulic heads in the confined aquifer fall below their historically lowest levels (Belitz and Phillips, 1995). For each climate change scenario, we simulate regional changes in confined heads as part of the hydrosalinity model in response to predicted future changes in groundwater pumping. Future occurrence of land subsidence was determined if time simulated confined heads fall would be below previously simulated minimum levels. We used an inelastic storage coefficient of 10%, i.e. 1 ft of subsidence for each 10 ft drop in head, to estimate total land subsidence in each grid cell over the period 2010-2100. We concluded that future land subsidence is limited, with no subsidence for wet scenarios and for the no-climate-change scenario. Some land subsidence (1 ft) was forecasted for the hadcm3-sresa1fi scenario.

6. Conclusions

The main conclusions on agricultural sustainability under climate change were:

- Water demand: Irrigation water demand does not change much due to compensating effects of rising temperature on evaporative demand and crop growth rate. In other words, an increase in reference ET is compensated by shorter growing seasons. This conclusion is robust for the wide range of climate change scenarios considered here. One consequence of shorter growing seasons could be that it will be possible to produce two crops each year. At that point irrigation water demand will increase significantly, perhaps beyond what can be supplied.

- Water supply: There is large uncertainty in future water supply under climate change, due to large variation in projected precipitation among climate change scenarios. Water supply estimates range from an increase of 10% to a decrease of 30% in 2100, compared to current conditions.

- Soil salinity: The spatial extent of salt-affected soils is projected to remain fairly stable in the 21st century for all climate change scenarios (except the one considering technological adaptation in the form of an improvement in irrigation efficiency: this scenario shows a decrease in salt-affected area). High soil salinity is limited to the eastern half of the study area, in where topography is low and flat, and soils are poorly drained. The western half of the study area is characterized by steeper topographic gradients and coarser alluvial deposits, which is why salinization due to rising water tables is unlikely to occur in those areas.

- Crop productivity: All scenarios project an increase in soil salinity in downslope areas, to the point where tomato and even cotton yields are negatively affected. Part of this area has already been retired from agricultural production, although model simulations indicate additional upslope areas may be affected. If no artificial drainage is possible on these lands, then additional land retirement may be the only option. Model results show that this process of continued salinization will occur regardless of climate change. This is especially significant given an anticipated demand-driven switch from salt tolerant crops (such as cotton) to high-value, salt-sensitive crops (such as tomato and melons).

- Groundwater salinity: Leaching of salts to groundwater mostly occurs in the western half of the study area (upslope), where soils are well drained. Over the long term, this could negatively impact salinity of underlying production aquifers, although this salinization process will take hundreds of years. Downslope areas on the other hand are characterized by groundwater discharge, resulting in upward salt fluxes from deeper groundwater into the root-zone, causing excessive soil salinization. Differences between scenarios in salt loading to groundwater are related to the amount of groundwater pumping.

- Land subsidence: Land subsidence is projected to be very limited, with no subsidence for wet scenarios and for the no-climate-change scenario. Greatest total land subsidence is projected to occur in the driest (hadcm3-sresa1fi) scenario, although the maximum simulated value is only 1 ft.

- Technological adaptation: One scenario considered technological adaptation in the form of an improvement of irrigation efficiency to 90%. If indeed technologically possible, this adaptation could effectively mitigate many adverse effects projected in all other climate change scenarios. It would reduce groundwater pumping, irrigation water demand, groundwater recharge, soil salinity (both extent and level of salinity), and would decrease the need for land retirement due to excessive soil salinization.

In summary, the greatest threat to agricultural sustainability in the area appears to be the continued salinization of downslope areas, which may jeopardize crop production and require further land retirement. Technological adaptation, such as improvements in irrigation efficiency, may be a possible way to mitigate these effects. Future work should consider additional scenarios, and evaluate the vulnerability of the system to further increases in groundwater pumping. Also, more work is needed on quantifying uncertainties in projected impacts, caused by not only uncertain climate projections, but also by uncertainties in the hydrosalinity model.

7. List of Publications

Ainsworth, E. A. and A. Rogers, 2007. The response of photosynthesis and stomatal conductance to rising CO_2: mechanisms and environmental interactions. Plant, Cell and Environment, 30:258–27.

Andreadis K.M. and Lettenmaier D.P., 2006, Trends in 20th century drought over the continental United States, Geophys. Res. Lett. 33 (10): L10403.

ASCE-EWRI, 2004, The ASCE standardized reference evapotranspiration equation, Technical Committee report to the Environmental and Water Resources Institute of the American Society of Civil Engineers from the Task Committee on Standardization of Reference Evapotranspiration, Reston ,VA, USA. 173 pp.

Belitz, K., S. P. Phillips, et al. (1993). Numerical simulation of ground-water flow in the central part of the western San Joaquin Valley, California. U.S. Geological Survey water-supply paper ; 2396. Washington, D.C., U.S. Geological Survey: vi, 69.

Cayan, D., E. Maurer, M. Dettinger, M. Tyree, K. Hayhoe, C. Bonfils, P. Duffy, and B. Santer, 2006. Climate scenarios for California, California Climate Change Center publication no. CEC-500-2005-203-SF.

Gordon, C., Cooper, C., Senior, C. A., Banks, H. T., Gregory, J.M., Johns, T.C., Mitchell, J.F.B. and R.A. Wood, 2002. The simulation of SST, sea ice extents and ocean heat transports in a version of the Hadley Centre coupled model without flux adjustments. Climate Dynamics 16: 147-168.

Hayhoe, K., D. R. Cayan, C. B. Field, P. C. Frumhoff, E. Maurer, N. Miller, S. Moser, S. Schneider, K. Cahill, E. Cleland, L. Dale, R. Drapek, R. M. Hanemann, L. Kalkstein, J. Lenihan, C. Lunch, R. Neilson, S. Sheridan and J. Verville, 2004. Emissions pathways, climate change, and impacts on California. Proceedings of the National Academy of Sciences 101(34): 12422–12427.

Howitt, R. E., M. Tauber, and E. Pienaar, 2003. Impacts of global climate change on California's agricultural water demand. Appendix X in PIER report.

IPCC, 2001. Climate Change 2001: Scientific Basis. Contribution of Working Group III to the Third Assessment Report of the Intergovernmental Panel on Climate Change. Edited by Bert Metz, et al. Cambridge, UK; New York, NY, USA: Published for the Intergovernmental Panel on Climate Change [by] Cambridge University Press.

Kalnay, E., et al., 1996: The NCEP/NCAR 40-year reanalysis project, Bull. Amer. Meteor. Soc., 77, 437-471.

Maurer, E.P., 2006, Uncertainty in hydrologic impacts of climate change in the Sierra Nevada, California under two emissions scenarios, Climatic Change (in revision).

Maurer, E.P., A.W. Wood, J.C. Adam, D.P. Lettenmaier, and B. Nijssen, 2002, A Long-Term Hydrologically-Based Data Set of Land Surface Fluxes and States for the Conterminous United States, J. Climate 15(22), 3237-3251.

Ritchie, J. T. and D. S. NeSmith, 1991. Temperature and crop development, p.5–29. In: J. Hanks and J. T. Ritchie (eds.), Modeling plant and soil systems. Agron. Monogr. 31, ASA, CSSA, and SSSA. Madison, WI.

Schoups G, Hopmans JW, Young CA, Vrugt JA, Wallender WW, Tanji KK, Panday S. 2005. Sustainabiliity of irrigated agriculture in the SJV, CA. PNAS 102(43):15352-6.

Shuttleworth, J.W., 1993, Evaporation, In: Handbook of Hydrology, D.R. Maidment, Ed., McGraw-Hill, Inc., 1424 pp.

Snyder, R. L., 1985. Hand calculating degree days. Agric. For. Meteorol., 35:353--358.

Snyder, R. L., B. J. Lanini, D. A. Shaw, and W. O. Pruitt, 1989. Using reference evapotranspiration and crop coefficients to estimate crop evapotranspiration for agronomic crops, grasses, and vegetable crops. California Department of Water Resources, Leaflet 21427, Sacramento, CA, pp. 1-12.

Vicuna, S. And Dracup, J.A. 2006. The evolution of climate change impact studies on hydrology and water resources in CA. Climatic Change.

Washington, W. M., Weatherly, J. W.; Meehl, G. A.; Semtner, A. J., Jr.; Bettge, T. W.; Craig, A. P.; Strand, W. G., Jr.; Arblaster, J.; Wayland, V. B.; James, R.; Zhang, Y., 2000, Parallel climate model (PCM) control and transient simulations. Climate Dynamics, Volume 16, Issue 10/11, pp. 755-774.

Wood, A.W., E.P. Maurer, A. Kumar and D.P. Lettenmaier, 2002. Long Range Experimental Hydrologic Forecasting for the Eastern U.S. J. Geophys. Res. 107 (D20): 4429,

Wood, A.W., L.R. Leung, V. Sridhar and D.P. Lettenmaier, 2004. Hydrologic implications of dynamical and statistical approaches to downscaling climate model outputs. Climatic Change 62: 189-216.

Yates D, D. Purkey, J. Sieber, A. Huber-Lee, and H. Galbraith, 2005, WEAP21 – A Demand-, Priority-, and Preference-Driven Water Planning Model, Part 2: Aiding Freshwater Ecosystem Service Evaluation, Water International 30 (4), 501–512.